The EMBO Journal (2012) 31, 4453–4465 | © 2012 European Molecular Biology Organization | All Rights Reserved 0261-4189/12
www.embojournal.org

THE EMBO JOURNAL

Nuclear export of histone deacetylase 7 during thymic selection is required for immune self-tolerance

Herbert G Kasler[1], Hyung W Lim[1], Denis Mottet[1,2], Amy M Collins, Intelly S Lee and Eric Verdin*

Gladstone Institute of Virology and Immunology, University of California, San Francisco, CA, USA

Histone deacetylase 7 (HDAC7) is a T-cell receptor (TCR) signal-dependent regulator of differentiation that is highly expressed in CD4/CD8 double-positive (DP) thymocytes. Here, we examine the effect of blocking TCR-dependent nuclear export of HDAC7 during thymic selection, through expression of a signal-resistant mutant of HDAC7 (HDAC7-ΔP) in thymocytes. We find that HDAC7-ΔP transgenic thymocytes exhibit a profound block in negative thymic selection, but can still undergo positive selection, resulting in the escape of autoreactive T cells into the periphery. Gene expression profiling reveals a comprehensive suppression of the negative selection-associated gene expression programme in DP thymocytes, associated with a defect in the activation of MAP kinase pathways by TCR signals. The consequence of this block *in vivo* is a lethal autoimmune syndrome involving the exocrine pancreas and other abdominal organs. These experiments establish a novel molecular model of autoimmunity and cast new light on the relationship between thymic selection and immune self-tolerance.
The EMBO Journal (2012) **31,** 4453–4465. doi:10.1038/emboj.2012.295; Published online 26 October 2012
Subject Categories: immunology
Keywords: autoimmunity; gene regulation; histone deacetylase; T-cell development; thymic selection

Introduction

The genetic basis of autoimmunity is only well understood for a few relatively rare syndromes (Nagamine *et al*, 1997; Bennett *et al*, 2001a). The search for novel molecular pathways that mediate self-tolerance is therefore an important part of understanding autoimmunity and devising new therapeutic strategies. Several mechanisms exist to insure T-cell self-tolerance. In the thymus, a complex process of clonal selection determines cell fate based on the strength of the interaction between the newly generated T-cell receptors (TCRs) of CD4/CD8 double-positive (DP) thymocytes and self antigens (Starr *et al*, 2003). If DP or more mature CD4 or CD8 single-positive (SP) thymocytes receive a TCR signal above a critical threshold, then they are either deleted or diverted into alternate lineages such as regulatory T cells (Tregs). However, this process of negative selection is insufficient to prevent autoimmunity. Autoreactive T cells that escape negative selection in the thymus must be suppressed, by both tolerogenic costimulatory receptors such as PD-1 and CTLA4 (Tivol *et al*, 1995; Keir *et al*, 2007) and Foxp3-expressing Tregs generated in the thymus and periphery (Hori *et al*, 2003).

All these mechanisms must function to maintain self-tolerance. A breakdown in any of them causes autoimmune disease in animal models (Ramsey *et al*, 2002; Hori *et al*, 2003; Fife and Bluestone, 2008), and also in humans (Nagamine *et al*, 1997; Bennett *et al*, 2001b). A common molecular theme among these mechanisms of T-cell self-tolerance is modulation of the developmental response to signalling through the TCR, through either cell-intrinsic changes associated with different developmental stages (as in thymic selection), or cell-extrinsic costimulatory and cytokine signals (as in peripheral tolerance and Treg generation). Mutations affecting the way TCR signals delivered in different contexts mediate developmental responses are therefore likely to be common among molecular lesions causing autoimmunity.

Some of the molecular elements linking TCR signalling to negative selection are known. These include the Bcl-2 family member Bim (Hildeman *et al*, 2002), the activity of JNK, ERK, and p38 MAP kinases (Rincon *et al*, 1998; Sugawara *et al*, 1998; Sabapathy *et al*, 2001; Daniels *et al*, 2006), the orphan steroid receptors Nur77 and Nor-1 (Woronicz *et al*, 1994; Calnan *et al*, 1995; Cheng *et al*, 1997) and recently Schnurri-2 (Staton *et al*, 2011). However, no 'master regulator' of the linkage between TCR signalling and negative selection in the thymus has been identified, and it is still unclear what switching mechanism can translate TCR signals of different affinities into different developmental outcomes.

Class IIa histone deacetylases (HDACs) such as HDAC7 are signal-dependent regulators of transcription that play important roles in multiple developmental processes. They are defined by a large non-catalytic N-terminal domain mediating recruitment to specific promoters and signal-dependent shuttling between the nucleus and the cytoplasm. The subcellular distribution of Class IIa HDACs is regulated by phosphorylation of conserved serine residues in this N-terminal regulatory domain (Grozinger and Schreiber, 2000; Wang *et al*, 2000; Kao *et al*, 2001; Parra *et al*, 2007). Phosphorylation of these residues leads to nuclear export and removal from target promoters (Grozinger and Schreiber, 2000; Lu *et al*, 2000; Wang *et al*, 2000; Kao *et al*, 2001; McKinsey *et al*, 2001). Mutation of these sites prevents nuclear export in response

*Corresponding author. Gladstone Institute of Virology and Immunology, University of California, 1650 Owens Street, San Francisco, CA 94158, USA. Tel.: +1 415 734 4808; Fax: +1 415 355 0855; E-mail: everdin@gladstone.ucsf.edu
[1]These authors contributed equally to this work.
[2]Present address: Metastasis Research Laboratory, GIGA—Cancer, Liege, Belgium.

Received: 25 January 2012; accepted: 2 October 2012; published online: 26 October 2012

to extracellular signals, and blocks signal-dependent differentiation events *in vitro* (Zhou *et al*, 2000; Kao *et al*, 2001). Thus, the class IIa HDACs regulate the expression of specific sets of developmentally important genes in response to extracellular signals causing their phosphorylation. Deletion of each of the individual class IIa HDACs *in vivo* interferes with important developmental processes (Zhang *et al*, 2002; Chang *et al*, 2004, 2006; Vega *et al*, 2004), as can expression of signal-resistant mutants (Zhang *et al*, 2002).

Previous evidence suggests a role for HDAC7 in thymic selection. HDAC7 is highly expressed in DP thymocytes and regulates the orphan steroid receptor Nur77, which plays a redundant role in negative selection (Woronicz *et al*, 1994; Calnan *et al*, 1995; Cheng *et al*, 1997; Dequiedt *et al*, 2003). In T-cell hybridomas, expression of a signal-resistant mutant of HDAC7 (HDAC7-ΔP), in which the serine residues that mediate TCR-dependent nuclear export have been mutated, suppressed apoptosis in response to TCR signals (Dequiedt *et al*, 2003). Conversely, thymus-specific deletion of HDAC7 results in excessive apoptosis of DP thymocytes, constitutive activation of MAP kinase pathways, and constitutive gene expression changes that normally occur only after TCR engagement (Kasler *et al*, 2011). In this work, we examine the effects of expression of HDAC7-ΔP specifically in thymocytes. We identify a key role for HDAC7 nuclear export in the process of negative selection *in vivo*, and define a novel molecular model of autoimmune disease.

Results

Blockade of HDAC7 nuclear export alters thymic T-cell development

To study the role of HDAC7 in thymic T-cell development, we employed a mutant HDAC7 lacking the phosphorylation sites required for TCR-dependent nuclear export (HDAC7-ΔP, Figure 1A). We introduced HDAC7-ΔP as a transgene in C57BL/6 (B6) mice, using p1013lcr, a vector containing the $p56^{lck}$ proximal promoter combined with the 3′ locus-controlling region of CD2 (Kasler *et al*, 2011). The pattern of expression mediated by p1013lcr approximates that of endogenous HDAC7, which is highly expressed from at least the DN3 stage through the DP stage, but declines through the SP stage and is nearly undetectable in lymph nodes (Kasler *et al*, 2011). For the experiments presented here, we chose transgenic lines that showed moderately elevated total HDAC7 expression in thymocytes, with near total disappearance of expression in peripheral lymph nodes (Supplementary Figure S1A).

HDAC7-ΔP expression affected the thymic CD4/CD8 profile, increasing the proportion of both CD4 and CD8 SP thymocytes to DP thymocytes (Figure 1B). Analysis of markers of positive selection and maturity in DP and SP thymocytes, including CD3ε, TCRβ, CD5, CD69, and CD24 (Figure 1C, see Supplementary Figure S1B and C for representative data), mostly revealed a bias towards a more mature phenotype in HDAC7-ΔP transgenic (HDAC7-ΔP TG) thymocytes, particularly in the CD8 SP population, which is composed of positively selected $CD3^{hi}$ CD8 SP thymocytes as well as CD3 negative immature single-positive cells (ISPs). One exception to this pattern was CD5, which is normally upregulated during positive selection, but was suppressed in all populations of HDAC7-ΔP TG thymocytes (Figure 1C; Supplementary Figure S1C). Enumeration of thymic cell populations revealed decreased cell numbers starting at the DN3-DN4 transition, followed by a further reduction at the ISP stage, followed by a rebound through the DP and SP stages (Figure 1D). The number of mature CD8 SP thymocytes in HDAC7-ΔP mice was approximately twice that of wild-type littermates, in spite of a 35% decrease in the average number of DP cells. Overall, this pattern suggested that while HDAC7-ΔP might hinder maturation through the β-selection checkpoint from the DN3 to ISP stages, it apparently facilitates maturation from the ISP stage through the SP stage. Numbers of both $CD4^+$ and $CD8^+$ T cells in the peripheral lymphoid organs were approximately normal (Figure1D).

While these results suggested that HDAC7-ΔP affects T-cell development, it was not clear if the effects were cell autonomous, or to what extent they might have been obscured by compensatory homeostatic mechanisms. We therefore evaluated the effect of HDAC7-ΔP expression on the competitive repopulation of mixed radiation chimeras. Equal numbers of wild-type (CD45.1/.2 heterozygous) and HDAC7-ΔP (CD45.2) bone marrow cells were transferred into lethally irradiated BoyJ (CD45.1) recipients. After 7–8 weeks, we examined the proportions of cells from each donor at different stages (for representative flow plots, see Supplementary Figure S1D).

In the common lymphoid progenitor, the contributions of HDAC7-ΔP and WT cells were nearly equal (Figure 1E). However, HDAC7-ΔP cells already appeared to be at a disadvantage at the DN1 stage. There was a further drop in the HDAC7-ΔP contribution through the DN3-DN4 and DN4-ISP transitions, reaching a minimum at the ISP stage. As observed in the transgenic animals, there was a substantial rebound through the DP and SP stages, particularly for CD8 SP cells. In contrast to what we observed in the transgenic animals, the contribution of HDAC7-ΔP cells in the peripheral lymphoid organs was markedly lower than that of WT cells, again particularly for the $CD8^+$ population. This suggested that either the competitiveness or the localization of T cells that had expressed HDAC7-ΔP during thymic selection was abnormal. Finally, we noted a substantial decrease in the proportion of $Foxp3^+$ T cells in the HDAC7-ΔP CD4 SP population in the thymus and in peripheral $CD4^+$ T cells (Supplementary Figure S1E and F), suggesting that HDAC7-ΔP significantly impaired the generation of Tregs. A similar decrease in $Foxp3^+$ T cells was observed in the transgenic animals (Supplementary Figure S1G). While less numerous, these cells suppressed T-cell activation in response to polyclonal activators normally (Supplementary Figure S2A).

HDAC7-ΔP blocks negative thymic selection more strongly than positive selection

We assessed the effect of HDAC7-ΔP on thymic selection in models of positive and negative selection involving the H-Y and OT-2 TCR transgenes. The H-Y TCR mediates negative selection in males, due to strong interaction with a Y-encoded ligand, but is positively selected in females (Bluthmann *et al*, 1988; Figure 2A). Expression of HDAC7-ΔP in H-Y males increased the number of both DP and CD8 SP thymocytes by ~100-fold (Figure 2A and B). This effect was observed in more than one line of HDAC7-ΔP X H-Y transgenic animals (Supplementary Figure S2D). In females, the effect of HDAC7-ΔP was more subtle, increasing the number of DP thymocytes

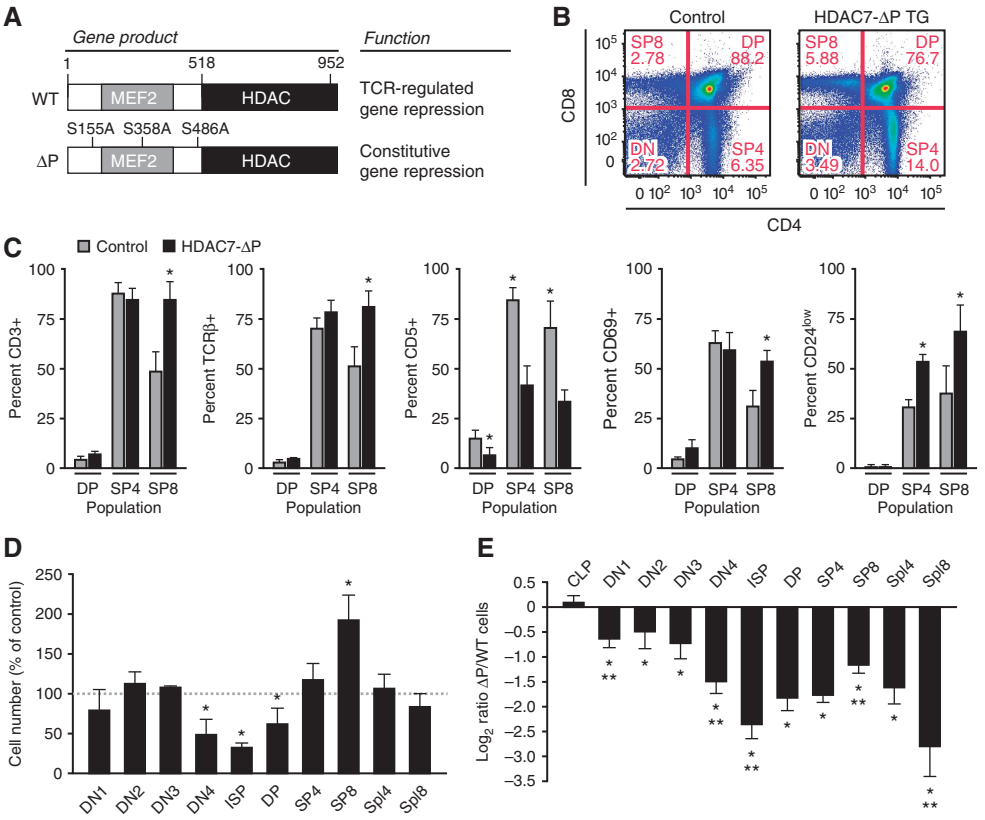

Figure 1 Expression of HDAC7-ΔP alters T-cell development. (**A**) Locations of S-A mutations in HDAC7-ΔP and the resultant alteration of HDAC7 function. (**B**) Representative scatter plots showing change in thymic CD4 and CD8 expression profiles in WT control (left) and HDAC7-ΔP TG (right) mice. (**C**) Effect of HDAC7-ΔP on expression of CD3ε, TCRβ, CD5, CD69, and CD24 in DP, CD4 SP, and CD8 SP thymocytes, gated as shown in Supplementary Figure S1C. Bars show percent ± s.d. for five control/HDAC7-ΔP TG littermate pairs. $*P = 6 \times 10^{-5} - 0.014$, two-tailed paired *T*-test. (**D**) Percent relative to WT littermate controls of cells present at the indicated developmental stages in HDAC7-ΔP TG mice. Data are from six control/HDAC7-ΔP TG littermate pairs ± s.e.m. $*P = 0.0057 - 0.039$, two-tailed paired *T*-test. (**E**) Log_2 ratio of WT/HDAC7-ΔP cells present at indicated stages in radiation chimeras reconstituted with equal amounts of wild-type control and HDAC7-ΔP bone marrow. Data are from eight animals engrafted with WT and transgenic bone marrow at a 1:1 ratio, ± s.e.m. $*P = 2.7 \times 10^{-9} - 0.026$ versus WT cells, two-tailed *T*-test; $**P = 0.001 - 0.04$ versus previous stage, two-tailed paired *t*-test. (**D**, **E**) CLP, common lymphoid progenitor; DN1-DN4, double-negative 1–4 thymocytes; ISP, immature single-positive; DP, CD4/CD8 double-positive; SP4, 8, CD4, 8 single-positive; Spl4, 8, spleen CD4, CD8 T cells.

by about two-fold without changing the number of CD8 SP cells (Figure 2A and B). A similar pattern was observed in the OT-2 TCR transgenic model, in which deletion can be induced by expression of ovalbumin (Figure 2A, Barnden *et al*, 1998). Expression of HDAC7-ΔP resulted in a 10-fold increase in the numbers of both DP and CD4 SP cells in OT-2 X act-Ova mice (Figure 2A and C), while causing a two-fold increase in DP cells and no change in CD4 SP cells in OT-2 mice not expressing Ova (Figure 2A and C). Thus, if the efficiency of negative selection is regarded as the number of DP and SP cells present and the efficiency of positive selection is regarded as the ratio of SP cells present to DP cells, HDAC7-ΔP causes a 10- to 100-fold decrease in the efficiency of negative selection and only a two-fold decrease in the efficiency of positive selection for these TCR transgenes. This interpretation is supported by examining the effect of HDAC7-ΔP on the DP/SP ratio in a polyclonal repertoire (Figure 1D and E). The overall increase in the SP/DP ratio caused by HDAC7-ΔP suggests that the defect in negative selection predominates over the defect in positive selection. Thus, thymocyte death in response to strong TCR signals appears to be strongly inhibited, while maturation the SP stage is only mildly impeded. The defect in thymocyte death appears to be specific to negative selection, as spontaneous apoptosis and death in response to dexamethasone treatment appear normal in HDAC7-ΔP TG thymocytes (Supplementary Figure S2B and C).

This apparent specific block in negative selection in HDAC7-ΔP TG thymocytes suggests that autoreactive thymocytes can escape to the periphery in these animals, a hypothesis that could be directly demonstrated in the case of the OT-2 X act-Ova system. In OT-2 X act-Ova X HDAC7-ΔP mice, we typically observed two-fold more CD4-positive and three-fold more CD4/Vα2-positive T cells than in OT-2 X act-Ova mice (Figure 2D and E). Consistent with this observation, in the polyclonal repertoire of peripheral T cells in WT: HDAC7-ΔP mixed radiation chimeras, expression of CD69 in the HDAC7-ΔP TG population was markedly elevated (Supplementary Figure S2E). Similarly, a substantially greater proportion of T cells from the HDAC7-ΔP population had an effector memory (i.e., $CD62L^{-}CD44^{+}$) phenotype (Supplementary Figure S2F), suggesting a more activated phenotype than their wild-type counterparts.

HDAC7 functions as a molecular 'safety switch' for the negative selection programme

To better understand the molecular basis of suppression of negative selection by HDAC7-ΔP, we examined the way that

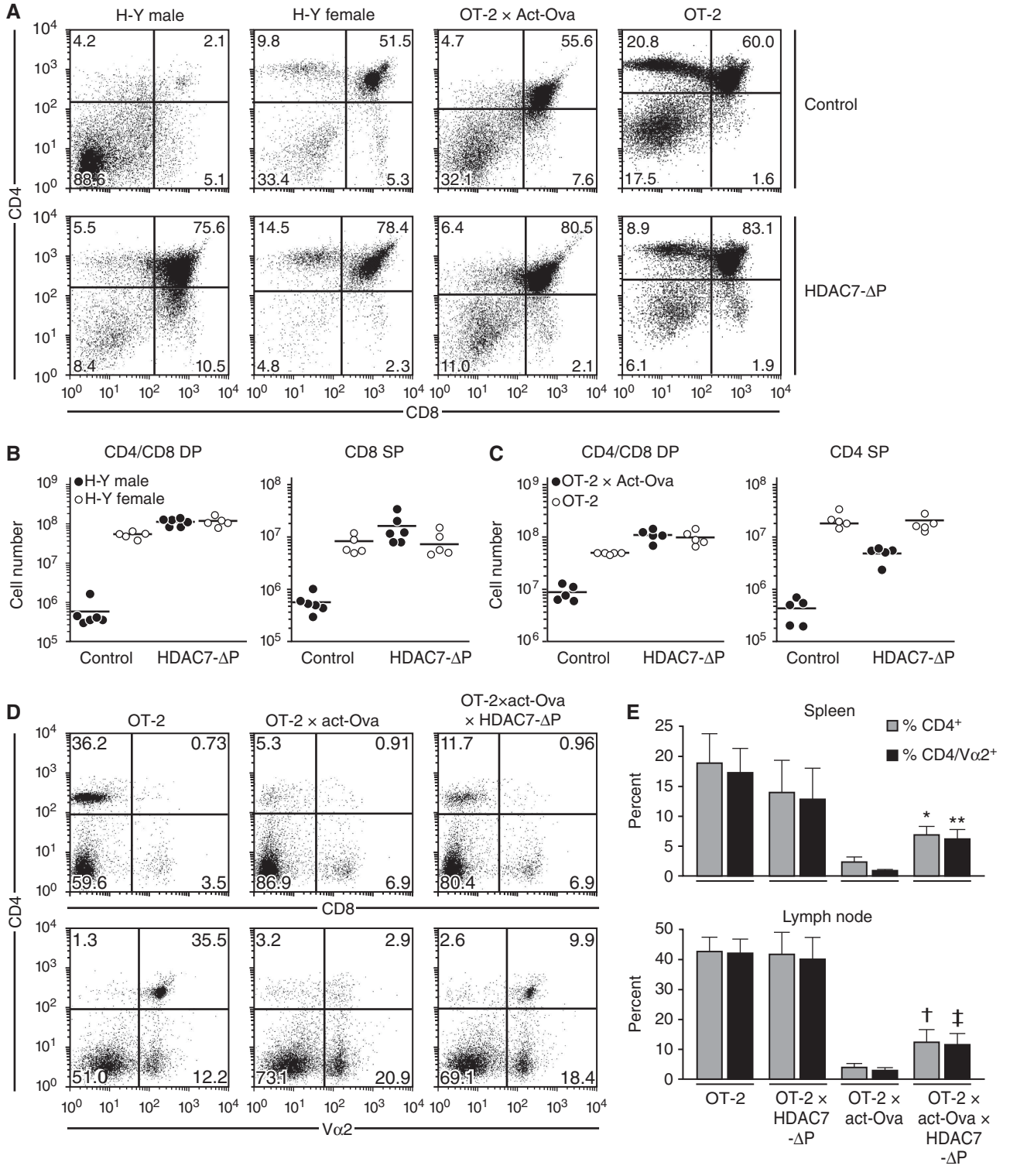

Figure 2 HDAC7-ΔP expression blocks negative thymic selection and permits escape of autoreactive T cells to the periphery. (**A**) Representative scatter plots showing CD4 and CD8 expression in male and female H-Y TCR transgenic mice (columns 1 and 2), as well as OT-2 X Act-Ova and OT-2 transgenic mice (columns 3 and 4) in the absence (top row) or presence (bottom row) of the HDAC7-ΔP transgene. (**B**) Quantification of CD4/CD8 DP (left) and CD8 SP (right) thymocytes in littermate male H-Y TCR and H-Y TCR X HDAC7-ΔP TG mice (filled circles), as well as the corresponding female mice (open circles). Results for five or six littermate pairs of control/HDAC7-ΔP TG mice are shown. *P*-values for WT-HDAC7-ΔP comparisons (two-tailed *T*-test) are as follows: male DP: 4.8×10^{-7}; female DP: 0.0023, male CD8 SP: 0.0032; female CD8 SP: 0.77. (**C**) Quantification of CD4/CD8 DP (left) and CD4 SP (right) thymocytes in OT-2 X act-Ova and OT-2 X act-Ova X HDAC7-ΔP TG mice (filled circles), as well as OT-2 and OT-2 X HDAC7-ΔP TG mice (open circles). Results are shown for five littermate pairs. *P*-values for WT-HDAC7-ΔP comparisons (two-tailed *T*-test) are as follows: OT2 X Act-Ova DP: 5.5×10^{-5}; OT-2 DP: 0.0038, OT2 X Act-Ova CD4 SP: 5.7×10^{-4}; OT2 CD4 SP: 0.51. (**D**) Representative scatter plots showing expression of CD4 versus CD8 (top) or CD4 versus Vα2 (bottom) in lymph nodes of OT-2 (left), OT-2 X Act-Ova (middle), and OT-2 X ACT-Ova X HDAC7-ΔP (right) mice. (**E**) Percent $CD4^+$ (dark grey) and $Va2^+$ (light grey) cells in spleen (top) and lymph node (bottom) of OT-2, OT-2 X HDAC7-ΔP, OT-2 X act-Ova, and OT-2 X HDAC7-ΔP X act-Ova mice. *P*-values for wt-HDAC7-ΔP comparisons (two-tailed *T*-test) are as follows: *0.00096; **0.0004; †0.0044; ‡0.003.

HDAC7-ΔP affects gene expression globally in thymocytes. Gene expression profiles were generated for OT-2 and OT-2 X HDAC7-ΔP TG DP thymocytes that had received negatively selecting TCR signals, 2.5 h after i.p. administration of their ovalbumin-derived cognate antigen (i.e., Ova stimulation). Comparison of the gene expression profiles from these Ova-stimulated thymocytes, both with one another and with previously generated expression profiles for wild-type and unstimulated OT-2 DP thymocytes (Kasler *et al*, 2011), yielded information about how HDAC7-ΔP affects gene expression changes associated with both positive and negative thymic selection (Figure 3A, see Supplementary Table S1 for a summary of differentially expressed genes in all comparisons).

Expression of HDAC7-ΔP in Ova-stimulated thymocytes had a broad suppressive effect on the gene expression programme normally associated with negative selection. This could be illustrated by plotting the gene expression changes normally occurring due to Ova stimulation (Figure 3B, horizontal axis) against the differences observed between Ova-stimulated OT-2 and OT-2 X HDAC7-ΔP thymocytes (Figure 3B, vertical axis). Genes that were induced by Ova stimulation were also highly likely to be suppressed by the expression of HDAC7-ΔP (Figure 3B, lower right quadrant). Conversely, genes normally suppressed by Ova stimulation were highly likely to be induced in HDAC7-ΔP X OT-2 thymocytes relative to their OT-2 counterparts (Figure 3B, upper left quadrant). This negative correlation is especially

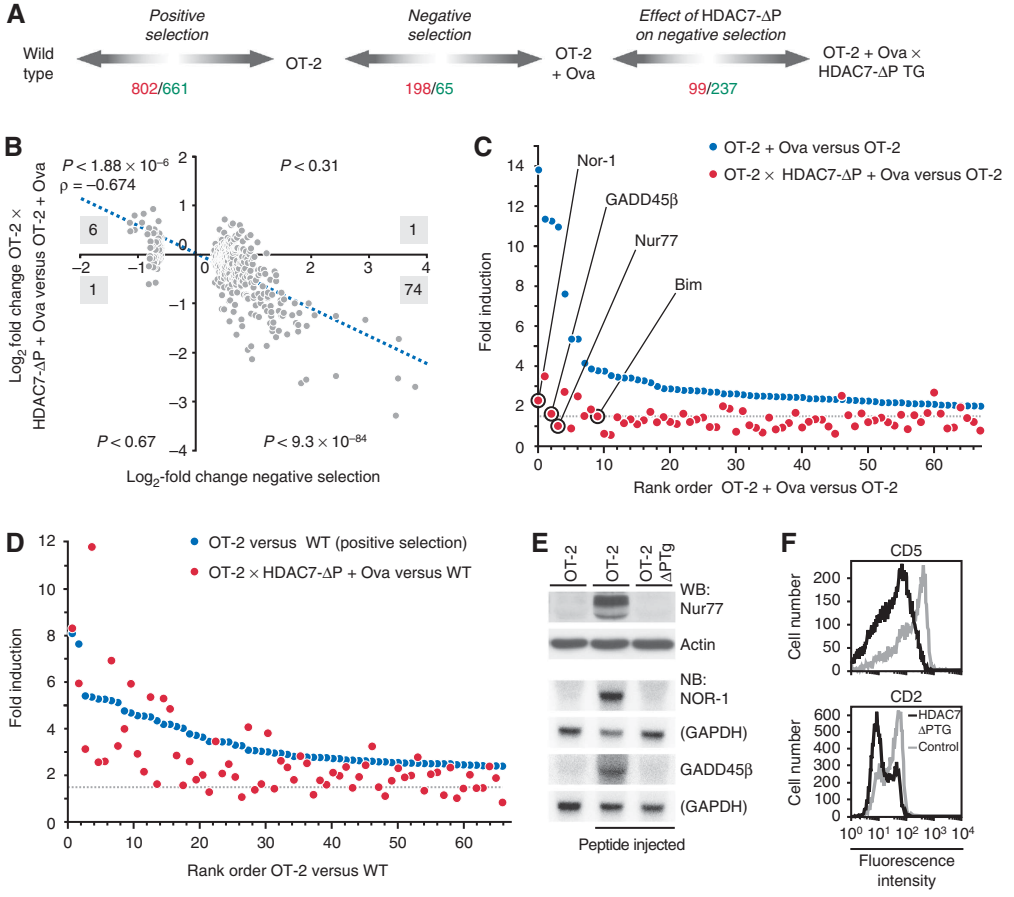

Figure 3 HDAC7-ΔP blocks some gene expression changes associated with positive selection and most gene expression changes associated with negative selection. (**A**) Diagram depicting DP thymocyte populations used for gene expression profiling and comparisons made to model positive selection, negative selection, and the effect of HDAC7-ΔP expression on gene expression during these processes. Numbers indicate how many genes were found to be significantly upregulated (red) and downregulated (green), based on a SAM delta score of ⩾1.85 and a mean fold differential expression ⩾1.5 for three biological replicates of each condition. (**B**) Scatter plot, with trend line and correlation coefficient indicated, showing gene expression changes during negative selection (OT-2 + Ova versus OT-2, horizontal axis) versus the corresponding differences between stimulated OT-2 and OT-2 X HDAC7-ΔP thymocytes (vertical axis). Results are shown for 263 genes found to be differentially expressed during negative selection, based on three littermate pairs of OT-2 and OT-2 X HDAC7-ΔP ova-injected mice. Black numbers indicate how many genes in each quadrant are differentially expressed for both comparisons. *P*-values shown for each quadrant are according to the binomial distribution for the number of overlapping genes indicated. (**C**) Graph showing fold upregulation of 67 genes upregulated two-fold or more in OT-2 DP thymocytes 2.5 h after agonist peptide injection versus unstimulated OT-2 thymocytes (blue symbols). Corresponding fold induction values are shown in red for OT-2 X HDAC7-ΔP TG DP thymocytes versus unstimulated OT-2 thymocytes. Dashed line indicates 1.5-fold threshold for significant induction. (**D**) Graph showing fold upregulation of top 67 genes induced during positive selection (OT-2 versus WT, blue symbols). Corresponding values are shown in red for Ova-stimulated OT-2 X HDAC7-ΔP TG DP thymocytes versus wild-type thymocytes. Dashed line indicates 1.5-fold threshold for significant induction. (**E**) Expression of Nur-77 (assayed by western blot), Nor-1, and GADD45β (assayed by northern blot) in OT-2 thymocytes (left), OT-2 thymocytes 2.5 h after antigenic peptide injection (middle), and OT-2 X HDAC7-ΔP TG thymocytes 2.5 h after antigenic peptide injection (right). (**F**) Expression of CD5 (top) and CD2 (bottom) in OT-2 (grey histograms) and OT-2 X HDAC7-ΔP TG (black histograms) DP thymocytes. Figure source data can be found with the Supplementary data.

strong for the genes most highly induced in negative selection. Of the 67 genes that were upregulated by two-fold or more after Ova treatment, only 15 were still significantly upregulated in HDAC7-ΔP X OT-2 thymocytes (Figure 3C, blue versus red symbols). Among the most highly induced genes that were strongly suppressed by HDAC7-ΔP were the death-inducing orphan steroid receptors Nur-77 and Nor-1, the BH3-only molecule Bim, which is required for negative selection, and the mediator of TCR-induced MAP kinase activation GADD45β (Figure 3C, circled symbols; Figure 3E).

This finding, that HDAC7 comprehensively regulates the gene expression programme associated with negative selection, seemed somewhat at odds with our prior findings concerning the effect of loss of HDAC7 in thymocytes (Kasler *et al*, 2011). In that study, we showed that HDAC7 is exported from the cell nucleus during positive selection, and that loss of HDAC7 resulted in the constitutive occurrence of gene expression changes in DP thymocytes that normally only occur after positive selection. However in the present study, we found that positive selection is the only modestly impaired in HDAC7-ΔP TG thymocytes (Figure 2A–C). We believe that the resolution to this discrepancy lies in the relative proportion of the gene expression changes associated with positive and negative selection that are affected by HDAC7. While over 75% of the gene expression changes that normally occur during negative selection do not occur in the presence of HDAC7-ΔP (Figure 3C), a significant but much smaller fraction of the changes that occur during positive selection are similarly affected. When we examined the top 67 genes induced during positive selection (OT-2 versus WT, Figure 3D, blue symbols), we found that only 21% of these were not induced in HDAC7-ΔP X OT-2 thymocytes versus wild-type thymocytes (Figure 3D, red symbols). Thus, while some gene expression changes clearly were suppressed (Figure 3D and F), they were apparently insufficient to block the entire process. It therefore appears that while nuclear export of HDAC7 largely mediates a change in gene expression that occurs during positive selection, that change is more critical for the execution of subsequent developmental programmes (e.g., negative selection) than for positive selection itself.

This dampening of the transcriptional response associated with negative selection suggests that in addition to directly regulating death mediators like Nur77, HDAC7-ΔP must also act high in the cascade of molecular events associated with TCR signalling. We previously observed changes in many genes involved in TCR signalling in thymocytes lacking HDAC7, and also an increase in the basal activity of p38, JNK, and Erk MAP kinases (Kasler *et al*, 2011). Conversely, when we examined the activation state of MAP kinases in peptide-stimulated OT-2 or OT-2, HDAC7-ΔP TG thymocytes at 3 h post injection, we saw strong suppression of the activation of p38 and Erk kinases at this time point (Figure 4A and B). To get a broader picture of how HDAC7-ΔP affects the activation of MAP kinases in thymocytes, as well as to rule out suppressive mechanisms involving defects in antigen-presenting cells or differences in the periphery, we examined the activity of P38 and Erk in OT-2 and OT-2 X HDAC7-ΔP DP thymocytes at different time points after *ex vivo* stimulation with α-CD3 and α-CD28 (Figure 4C–E). While there was some activation of P38 and Erk observable in HDAC7-ΔP thymocytes in this format, P38 activity was significantly reduced at all time points (Figure 4D), While Erk activity was significantly reduced at 100 and 150 min (Figure 4E). Splenic $CD4^+$ T cells from these animals were also activated *ex vivo*, using autologous APC and Ova peptide, and upregulation of CD69 and CD25, as well as the ability to dilute CFSE, were normal in the CD4 T cells of the OT-2 X HDAC7-ΔP animals (Supplementary Figure S2G and H). The activation of both P38 and Erk kinases has been implicated in the negative selection of autoreactive thymocytes (Sugawara *et al*, 1998; Daniels *et al*, 2006), so it is likely that the ability of HDAC7-ΔP to block their activation in response to TCR ligation is an important component of its broad suppression of the negative selection programme. In summary, our observations suggest that HDAC7 regulates a functional cassette of genes during positive selection that are required to enable the Erk and p38 MAP kinase pathways to respond appropriately to negatively selecting TCR signals. In addition to this mode of action, HDAC7 also directly represses pro-apoptotic genes like Nur-77 that are not strongly induced during positive selection but require nuclear exclusion of HDAC7 in order to be induced during negative selection (Dequiedt *et al*, 2003).

HDAC7-ΔP TG mice develop lethal multi-organ autoimmunity

Monitoring the health of the HDAC7-ΔP TG mice, we found that from 5 weeks to 6 months of age, ~80% of HDAC7-ΔP mice ceased to thrive, lost weight (Figure 5A), and became moribund (Figure 5B). Gross pathologic examination of the sick animals revealed a greatly distended digestive tract (Figure 5C), filled with abnormal faecal material. Staining of the faecal pellets with Sudan IV demonstrated steatorrhea (Figure 5D). Histologic examination of the pancreas in these animals revealed obliteration of the exocrine areas, with the islets remaining largely intact (Figure 5E).

Leukocytic infiltrates were frequently observable in histologic sections (Figure 5F). Staining of infiltrating cells from the pancreatic tissue showed the abnormal presence of B cells, $CD4^+$, and $CD8^+$ T cells (Figure 5G). Auto-antibodies to pancreas were also present in the sera of nearly all sick HDAC7-ΔP TG animals, which could be demonstrated by reactivity against sections of pancreatic tissue (Figure 6A) and also by western blot (Supplementary Figure S3A). While clinically prominent, exocrine pancreatitis was not the only disease observed in HDAC7-ΔP TG mice. Western blotting revealed autoantibodies specific for a broad array of tissues (Figure 6B; Supplementary Figure S3B), and histologic examination revealed the frequent presence of destructive leukocytic infiltrates in the stomach and liver (Figure 6C). Importantly, expression of HDAC7-ΔP on a lymphocyte-deficient ($Rag1^{-/-}$) background abrogated this pathology. These animals neither lost weight nor died at a greater frequency than littermate non-transgenic Rag1-deficient animals (Figure 6D; Supplementary Figure S3C), indicating that lymphocytes were required for autoimmunity.

Autoimmunity can be dominantly transferred by HDAC7-ΔP bone marrow or peripheral T cells

Beyond demonstrating the requirement for lymphocytes, further experiments were required to specifically tie autoimmunity in HDAC-ΔP mice to the defect in thymic negative selection, rather than other possible mechanisms. Ruling out

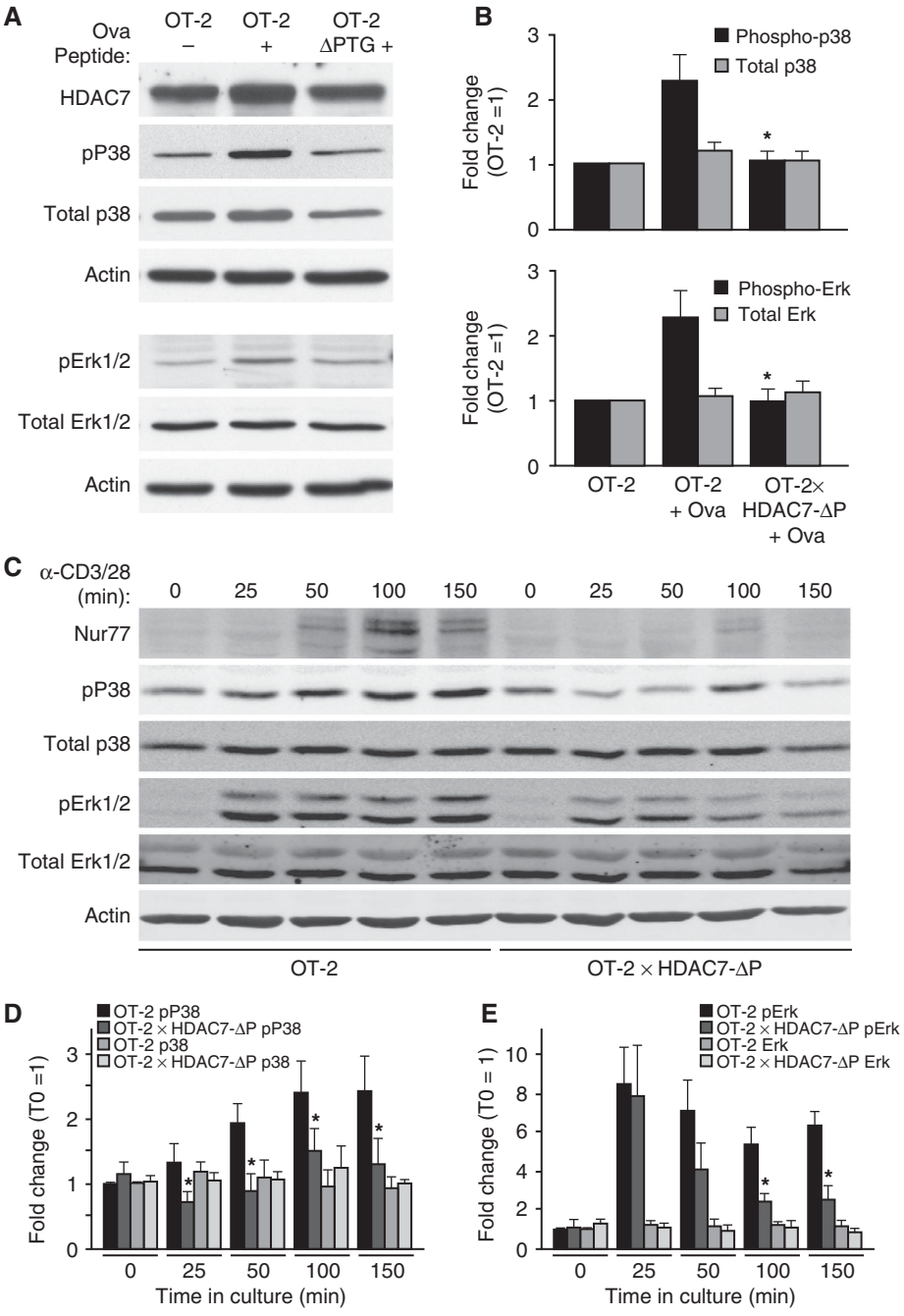

Figure 4 HDAC7-ΔP blocks MAP kinase activation after strong TCR engagement. (**A**) Representative western blot showing phospho-p38, total p38, phospho-Erk1/2, total Erk1/2, HDAC7, and Actin expression for unstimulated OT-2 DP thymocytes (left), OT-2 DP thymocytes 3 h after agonist peptide injection (middle), and HDAC7-ΔP X OT-2 DP thymocytes 3 h after agonist peptide injection (right). (**B**) Quantification by optical densitometry of phospho- and total p38 (top), and Erk (bottom) for DP thymocytes from four sets of animals prepared as in (**A**). $^*P = 0.008$–0.028 for stimulated OT-2 X HDAC7-ΔP versus stimulated littermate OT-2 thymocytes, two-tailed *T*-test. (**C**) Representative western blots showing expression of Nur77, phospho-P38, total P38, phospho-Erk, total Erk, and actin for OT-2 and OT-2 X HDAC7-ΔP DP thymocytes stimulated *ex vivo* with α-CD3 + α-CD28 for the indicated times. (**D**) Fluorimetric quantification of phospho- and total P38 in OT-2 and OT-2 X HDAC7-ΔP DP thymocytes stimulated with α-CD3 + α-CD28 for the indicated times. $^*P = 0.0006$–0.027, paired two-tailed *T*-test. (**E**) Fluorimetric quantification of phospho- and total Erk in OT-2 and OT-2 X HDAC7-ΔP DP thymocytes stimulated with αCD3 + αCD28 for the indicated times. $^*P = 0.0012$–0.013, paired two-tailed *T*-test. Figure source data can be found with the Supplementary data.

mechanisms involving Tregs was particularly important, since we did observe some deficiency in the thymic generation of Tregs (Supplementary Figure S1E–G), and autoimmunity similar to what we observed has been elicited by mutations models impairing both negative selection and Treg function (Niki *et al*, 2006; Meagher *et al*, 2008). Other alternative mechanisms such as a defect in antigen presentation or some abnormality in B cells also needed to be ruled out. We therefore set up adoptive transfer experiments, in which splenic lymphocytes from HDAC7-ΔP TG or WT littermate mice were transferred into Rag1-deficient hosts. All recipients received wild-type B cells,

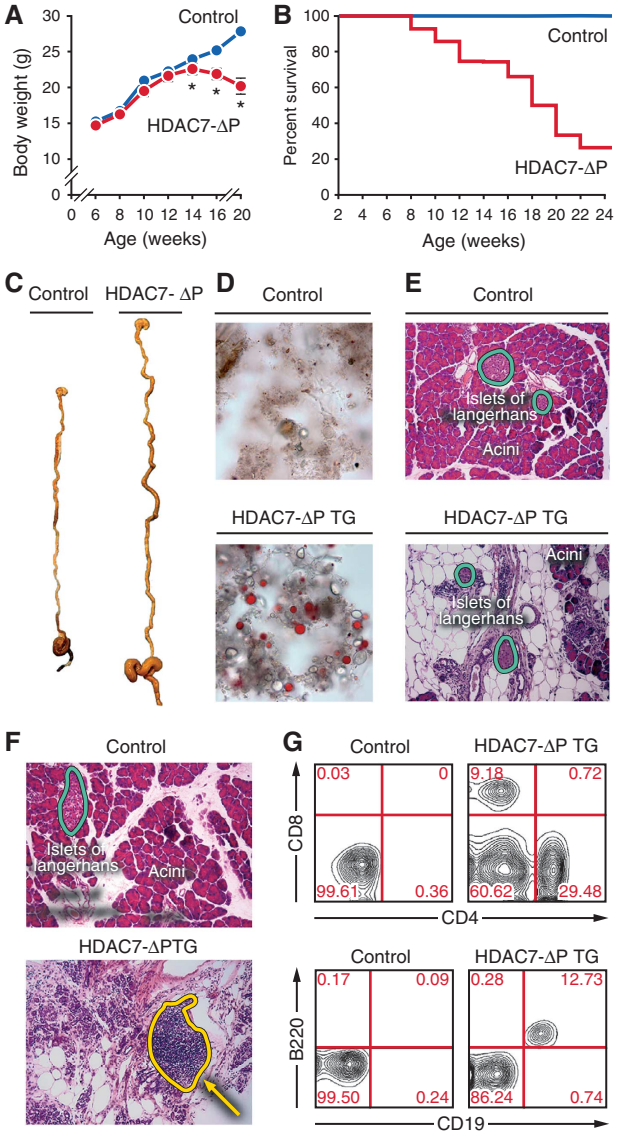

Figure 5 Thymic expression of HDAC7-ΔP causes lethal exocrine pancreatitis. (**A**) Body weight in grams of WT and HDAC7-ΔP TG animals between 6 and 20 weeks of age. Values are mean ± s.e.m. of eight transgenic animals and corresponding WT littermates. $^{*}P<0.01$, two-tailed *T*-test. (**B**) Percent survival of cohorts of eight HDAC7-ΔP TG and eight WT littermate animals from 2 to 24 weeks of age. (**C**) Representative gross specimens of WT littermate (left) and HDAC7-ΔP TG (right) digestive systems from animals 14 weeks of age. (**D**) Representative Sudan IV-stained faecal smear micrographs from WT littermate control (top) and HDAC7-ΔP TG (bottom) mice, demonstrating steatorrhea in HDAC7-ΔP TG animals. (**E**) Representative haematoxylin and eosin stained sections of WT (top) and HDAC7-ΔP TG (bottom) pancreas, showing massive destruction of acinar tissue but not islets in HDAC7-ΔP TG animals. (**F**) Representative haematoxylin and eosin stained sections of wild-type littermate control (top) and HDAC7-ΔP TG (bottom) pancreas, showing extensive immune infiltrate in HDAC7-ΔP TG specimen (dotted yellow outline). (**G**) Representative scatter plots measuring CD4 and CD8 (top) or CD19 and B220 expression (bottom) in pancreatic infiltrate cells from wild-type littermate control (left) and HDAC7-ΔP TG (right) mice.

alone or together with wild-type T cells, HDAC7-ΔP T cells, or a 1:1 mixture of WT and HDAC7-ΔP T cells. Both groups that received HDAC7-ΔP T cells died at a higher frequency than those that received no T cells or WT T cells only (Figure 6E). The animals receiving HDAC7-ΔP T cells also developed steatorrhea and lost weight, in contrast to those that received no or only wild-type T cells (Supplementary Figure S3D and E).

These experiments demonstrated that peripheral T cells from HDAC7-ΔP T mice were sufficient to induce autoimmunity, and also suggested that wild-type Tregs were not able to rescue the phenotype. However, defects in T-cell homeostasis, due to lymphopenia resulting from the developmental disadvantages of HDAC7-ΔP T cells, might still have caused autoimmunity that could not be readily suppressed by the normal regulatory cells co-transferred into Rag1-deficient recipients. Alternatively, defects in thymic antigen presentation rather than intrinsic defects in the response of thymocytes to TCR signalling may have been responsible for the negative selection defect. To rule out these mechanisms, we evaluated the effect of HDAC7-ΔP haematopoietic stem cells in mixed radiation chimeras. We determined that a 1:5 or 1:10 ratio of WT: HDAC7-ΔP bone marrow cells was optimal to produce a 1:1 ratio of peripheral T cells derived from these lineages (Figure 7A). Cohorts were established that received WT and HDAC7-ΔP bone marrow cells at these ratios, as well as mice reconstituted solely with WT cells. Examining the ratio of Tregs to conventional T cells in a broad collection of peripheral T cells from these animals, we saw no significant difference between the WT-only and 1:5 WT: HDAC7-ΔP chimeras (Supplementary Figure S3F).

Within 8 weeks of engraftment, mice that had received HDAC7-ΔP bone marrow began to lose weight, and by 20 weeks post engraftment, 5/8 of the 1:5 and 7/8 of the 1:10 chimeras had either died or become moribund (Figure 7B and C). As expected, histologic examination of the 1:5 chimeras revealed severe autoimmune destruction of the exocrine pancreas, as well as destructive immune infiltrates in the liver (Figure 7D). Finally, examination of pancreas-infiltrating cells in a separate cohort of 1:5 WT: HDAC7-ΔP chimeras showed that the infiltrates were predominantly composed of $CD8^{+}$ T cells derived from HDAC7-ΔP donor (Figure 7E), suggesting that autoimmune attack was mediated only by the T cells expressing HDAC7-ΔP. These results provided strong evidence that the profound defect in negative selection caused by blockade of HDAC7 nuclear export in thymocytes is sufficient to lead to lethal autoimmunity affecting multiple organ systems.

Discussion

In this work, we show that nuclear export of HDAC7 functions as a TCR-dependent genetic switch controlling the transcriptional programme associated with negative thymic selection. Thymocytes expressing the signal-resistant HDAC7 mutant HDAC7-ΔP can undergo positive selection, but fail to be deleted in response to strong TCR engagement and instead escape to the periphery, causing lethal autoimmune disease. The generation of Tregs is also impaired in HDAC7-ΔP TG thymocytes, but this block is not as categorical as the block in negative selection, and the defect in Treg generation is not dominant in the induction of autoimmunity. The specificity of HDAC7 as a gatekeeper for the genetic programme mediating negative selection is indicated by the very broad manner in which induction of the major known mediators of deletion is suppressed by HDAC7-ΔP.

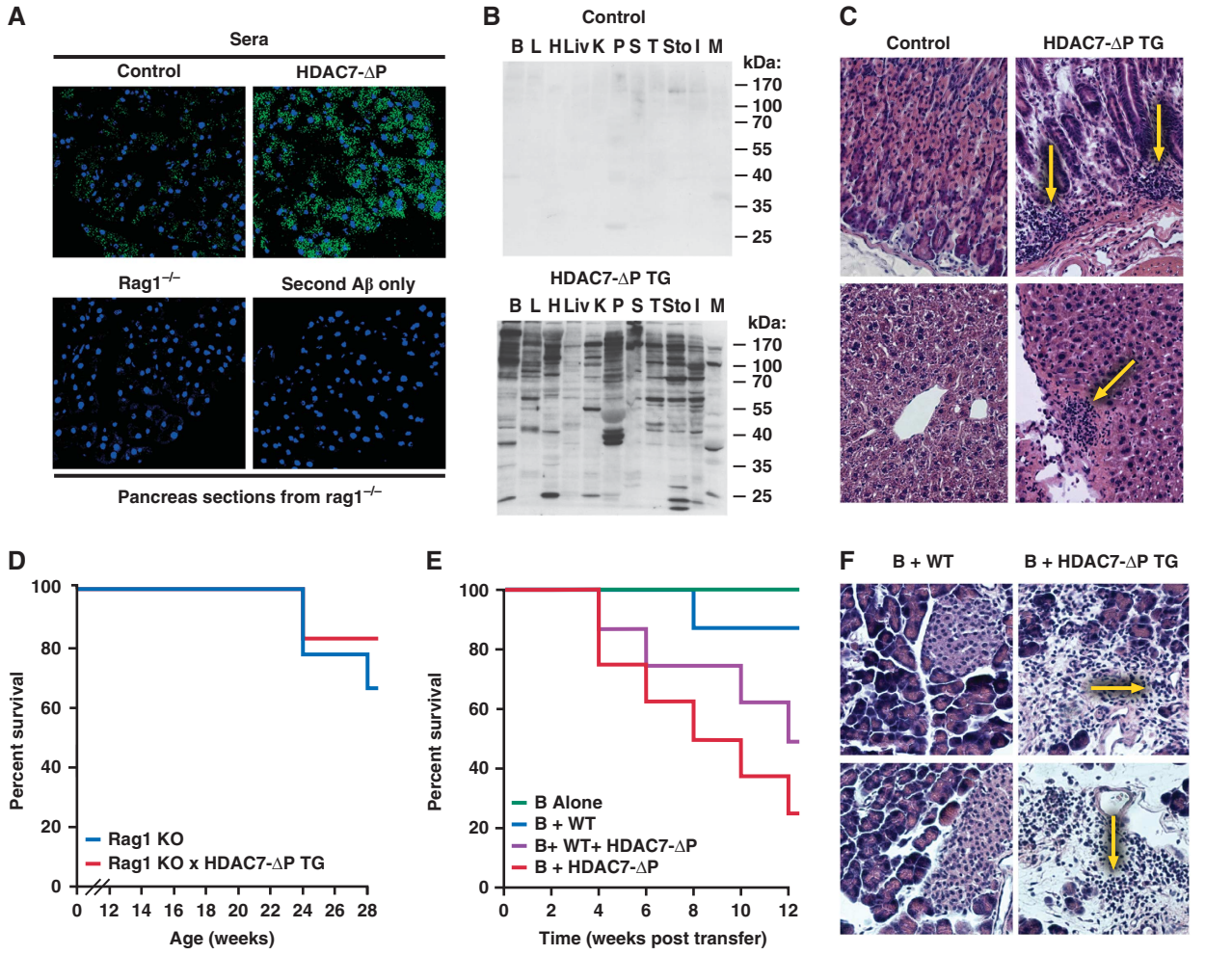

Figure 6 Thymic HDAC7-ΔP expression causes multi-organ visceral autoimmunity. (**A**) Immunofluorescence staining of pancreatic sections from Rag1-deficient mice with sera from wild-type littermate control (top left) and HDAC7-ΔP TG (top right) sera. Bottom left shows reactivity of rag1 KO sera, bottom right signal from incubation with secondary antibody only. (**B**) Representative western blots showing reactivity of wild-type littermate control (top) and HDAC7-ΔP TG (bottom) serum against a panel of whole tissue extracts from Rag1-deficient animals. (**C**) Representative haematoxylin and eosin stained sections of wild-type control (left) and HDAC7-ΔP TG (right) stomach (top) and liver (bottom), showing immune infiltrates and local tissue damage (yellow arrows). (**D**) Percent survival of cohorts of six Rag1 KO littermate control (blue line) and six Rag1 KO/HDAC7-ΔP TG mice (red line) from 12 to 26 weeks of age. (**E**) Percent survival from 0 to 12 weeks post transfer of four cohorts of eight Rag1 KO mice transferred with wild-type B cells and T cells from WT and HDAC7-ΔP TG mice as indicated in legend. (**F**) Representative haematoxylin and eosin stained sections of pancreas from two mice engrafted with wild-type T and B cells (left) and two HDAC7-ΔP T+wild-type B cell-engrafted mice (right), showing destructive infiltrates in the mice receiving HDAC7-ΔP T cells (yellow arrows).

While HDAC7 apparently suppresses the transcriptional programme associated with negative selection, prior studies of its thymic function indicate that its nuclear export occurs during positive rather than negative selection, and many of the genes it regulates show expression changes during that process (Kasler *et al*, 2011; Figure 3D). It thus appears that HDAC7 nuclear export mediates a change in gene expression during positive selection that is required for negative selection. DP cells with enforced nuclear HDAC7 appear to have fewer developmental options than DP cells with cytoplasmic HDAC7, suggesting that HDAC7 nuclear export is required to enable the next set of developmental choices for thymocytes that have been positively selected (Figure 7F). The molecular mechanisms underlying this developmental effect include both the direct repression of pro-apoptotic genes like Nur-77 and a broad dampening effect on the gain of the TCR signalling pathway with respect to activating downstream effectors like MAP kinases. Supporting the latter mechanism, a recent study has shown that expression of HDAC7-ΔP in mature CD8 T cells strongly suppresses their activation and function as cytotoxic T effectors (Navarro *et al*, 2011). Once HDAC7 is lost from the nucleus, thymocytes become more prone to apoptosis, an effect that is strongly evident when HDAC7 is deleted from thymocytes (Kasler *et al*, 2011). Its nuclear localization prior to positive selection may thus represent an important 'safety' mechanism that prevents transient stochastic excitations of the TCR pathway from prematurely causing negative selection of DP thymocytes.

From a molecular standpoint, a noteworthy aspect of the effect of HDAC7-ΔP in thymocytes is the suppression of p38 and Erk kinase activation in response to strong TCR signals. These MAP kinase modules are implicated in the life/death decision during thymic selection (Sugawara *et al*, 1998; Daniels *et al*, 2006), and the broad importance of these pathways in regulating cellular response programmes is consistent with the categorical role that HDAC7 plays thymic

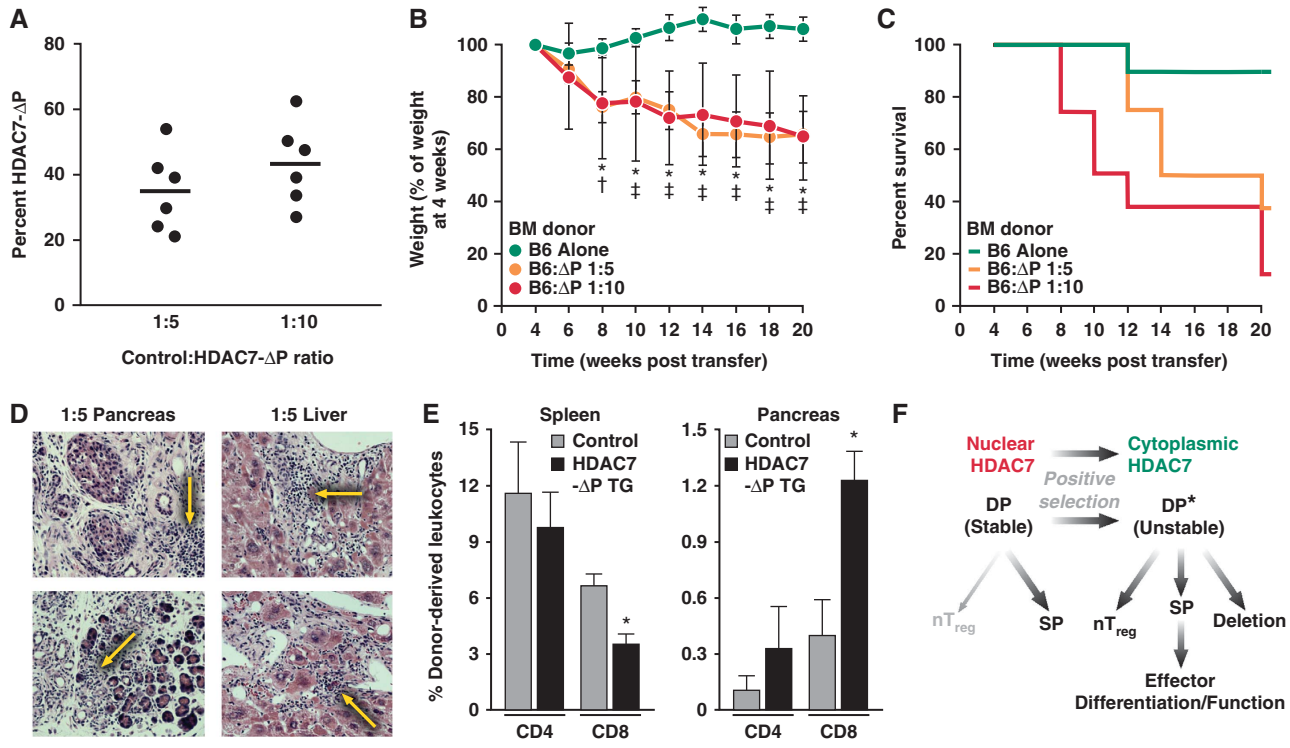

Figure 7 Autoimmunity mediated by HDAC7-ΔP is dominantly transferable in mixed radiation chimeras. (**A**) Percentage of cells from HDAC7-ΔP TG donors present in circulating T cells in 1:5 and 1:10 WT:HDAC7-ΔP radiation chimeras. Blood was taken 6 weeks after engraftment. (**B**) Mean weights (in % of weight at 4 weeks post engraftment) of three cohorts, each of eight irradiated BoyJ recipients, engrafted as indicated with WT and HDAC7-ΔP TG bone marrow, from 4 to 20 weeks post engraftment. $^{*}P = 0.0005$–0.0057, two-tailed *T*-test, WT:HDAC7-ΔP BM at 1:10; $^{\dagger}P = 0.02$, two-tailed *T*-test, WT:HDAC7-ΔP BM at 1:5. $^{\ddagger}P = 7.0 \times 10^{-5}$–$0.013$, two-tailed *T*-test, WT:HDAC7-ΔP BM at 1:5. (**C**) Percent survival over the same interval of time for the cohorts described in (**B**). (**D**) Representative haematoxylin and eosin stained sections of pancreas (left) and liver (right) from two 1:5 WT:HDAC7-ΔP chimeras, showing immune infiltrates and tissue destruction (yellow arrows). (**E**) Mean percentages of pancreas-infiltrating CD4 and CD8 T cells derived from WT donors, HDAC7-ΔP TG donors, or recipients for five 1:5 WT:HDAC7-ΔP radiation chimeras 10 weeks post engraftment. $^{*}P = 0.02$ for spleen, 0.004 for pancreas, paired two-tailed *T*-test, for WT versus HDAC7-ΔP populations in the same animal. (**F**) Diagram depicting model of HDAC7 function in thymic selection, in which nuclear export of HDAC7 destabilizes the signalling network of DP thymocytes during positive selection and enables subsequent developmental programmes.

selection. It is likely that this mechanism of action is involved in other developmental programmes that are enabled by class IIa HDACs. For example, cardiac hypertrophy and type II diabetes are processes that are regulated both by Class IIa HDACs (Mihaylova *et al*, 2011; Wang *et al*, 2011) and also by MAP kinases (Peter *et al*, 2007; Gehart *et al*, 2010).

The activity of MAP kinases is also critical for the activation of peripheral T cells, and the finding that constitutive nuclear localization of HDAC7 suppresses CD8 effector function suggests that HDAC7 may play a role in regulating T-cell activation in the periphery as well as the thymus (Navarro *et al*, 2011). Since the localization of HDAC7 in most cells appears to be cytoplasmic from the SP thymocyte stage forward, regardless of TCR signalling (Kasler *et al*, 2011; Navarro *et al*, 2011), a key question in investigating the possibility of this mechanism will be what extracellular signals might drive it back into the nucleus in mature T cells. One particularly compelling finding in this regard is that the cAMP-PKA pathway promotes dephosphorylation and nuclear localization of class IIa HDACs, thus suppressing insulin signalling (Mihaylova *et al*, 2011; Wang *et al*, 2011). This pathway has long been known to exert a repressive effect on T-cell activation and function (Mosenden and Tasken, 2011), so the notion that nuclear localization of HDAC7 or another class IIa HDAC via this pathway may contribute somehow to the suppression of peripheral immune responses is intriguing. Future studies in our laboratory and others will no doubt help resolve these possibilities.

From a cellular standpoint, these studies shed new light on the relationship between thymic selection and immune self-tolerance. The two main extant physiologic models of autoimmunity that are due to defects in negative thymic selection are deficiency of Bim and deficiency of AIRE (Bouillet *et al*, 2002; Anderson *et al*, 2005a, b). NOD mice, which develop type 1 diabetes later in life, also show a broad dampening of the transcriptional programme associated with negative selection (Zucchelli *et al*, 2005); however, there are multiple models of how autoimmunity is initiated in the NOD strain. Each of these strains in which negative selection is impaired exhibits a different autoimmune phenotype. Deficiency of Bim, which results in a profound block in apoptosis of autoreactive thymocytes (Bouillet *et al*, 2002), results in a Lupus-like syndrome that has a slower onset than autoimmunity in HDAC7-ΔP TG mice (Bouillet *et al*, 1999). This becomes substantially more fulminant and lethal if the Fas death receptor is also deleted (Hutcheson *et al*, 2008; Weant *et al*, 2008). Deficiency of AIRE, which is required for the presentation of peripheral antigens to SP thymocytes in the thymic medulla, results in an apparently broader tissue

distribution of autoimmune infiltrates than expression of HDAC7-ΔP in thymocytes, but with less lethality (Anderson *et al*, 2002). Remarkably, combining the AIRE$^{-/-}$ and NOD genotypes results in a syndrome that has some resemblance what we observe in our model, with exocrine pancreatitis also representing the dominant clinical feature (Niki *et al*, 2006). Further experiments, particularly combining HDAC7-ΔP with these genotypes, will be required to resolve the epistatic relationships between these genetic lesions. The question of why such a strong block in negative selection, elicited either by expressing HDAC7-ΔP or by combining loss of AIRE with other mutations affecting this process, should show an altered or restricted tissue distribution relative to negative selection of AIRE alone will also require further investigation. Again, combining HDAC7-ΔP expression with other lesions affecting negative selection and investigating its effects in different background strains will most likely prove informative. Lastly, although these studies elucidate a clear nuclear mechanism of action for HDAC7 in thymocytes, they do not address what function it may have in the cytoplasm, since the endogenous HDAC7 in HDAC7-ΔP TG animals is exported from the nucleus normally.

The observation that perturbing HDAC7 function in thymocytes can cause lethal autoimmunity opens up new signalling pathways as potential targets in the treatment of human autoimmune disease. Although autoimmune exocrine pancreatitis is a minor human clinical entity, differences in genetic background, even within the same species, can have strong effects on what tissues come under attack. Thus, human syndromes distinct from what we have observed in B6 mice may be related to HDAC7. In addition to polymorphisms in HDAC7 itself, defects in the multiple pathways that regulate its nuclear versus cytoplasmic localization in different cellular contexts may be among human mutations that cause autoimmunity. Based on what we have observed, a defect in the proximal TCR signalling apparatus that somehow selectively affects class IIa HDAC nuclear export in thymocytes might be a potent inducer of autoimmunity. Recent findings that attenuation of the function of proximal elements in the TCR signalling pathway, such as Zap-70, can lead to autoimmunity (Tanaka *et al*, 2010) are particularly encouraging in this regard, and will greatly inform our future efforts to better understand the possible role of HDAC7 in the genetics of human autoimmune disease.

Materials and methods

Mouse strains

All experimental strains were on a C57BL/6 (B6) genetic background. B6, BoyJ, OT-2, and Rag1$^{-/-}$ mice were obtained from Jackson Laboratories, and H-Y mice from Taconic Farms. Mice expressing the HDAC7-ΔP transgene were prepared by pronuclear injection of p1013 LCR-HDAC7-ΔP into B6 recipients following standard protocols. P1013 LCR is described elsewhere (Kasler *et al*, 2011). The coding sequence for HDAC7-ΔP (Human HDAC7, with the mutations S155A, S358A, and S486A) was inserted into the *Bam* H1 site of p1013LCR.

Antibodies

Antibodies used for western blotting were as follows: HDAC7: H-273 rabbit polyclonal (Santa Cruz Biotech); β-actin: C-4 (MP Biomedicals); phospho-Erk: D13.14.4E (Cell Signaling); Phospho-p38: rabbit polyclonal cat # 9211 (Cell Signaling); Erk: 3A7 (Cell Signaling); P38: rabbit polyclonal cat # 9212 (Cell Signaling). Antibodies used for flow cytometry and cell sorting were as follows: CD4: GK1.5, fluorescein isothiocyanate (-FITC), phycoerythrin (-PE), or Alexa-Flour 647 (-AF647)-conjugated (UCSF hybridoma core facility); CD8α: YTS169.4-AF647 (UCSF HCF), PerCP (BioLegend), or 53-6.7-PE (BD); CD3ε: 145-2C11-FITC, PE-Cy7 (UCSF HCF), or -APC (BD); CD44: IM7.8.1-FITC (Invitrogen); CD24: 30-F1-PE (eBioscience); CD25: 3C7-PE (BD); CD2: RM2-5-FITC (BD); CD5: 53-7.3-APC (eBioscience); CD62L: MEL-14-PE (BD); CD147: RL73-PE (eBioscience); CF11b (Mac-1): M1/70-APC (eBioscience); Ly-6G (Gr-1): RB6-8C5-APC (eBioscience); Ter-119: TER-119-APC (eBioscience); NK1.1: clone PK136-APC (eBioscience); control rat IgG_1: R3-34-PE (BD); CD45.1: A20.1-7-A647 (UCSF HCF); CD45.2: clone 104-PerCP (Biolegend); TCRβ: H57-597-APC-eFluor780 (eBioscience); Vα2: B20.1-biotin (eBioscience). PE-conjugated, α-galCer-loaded CD1d tetramers were obtained from Proimmune LLC.

Flow cytometry

Cell suspensions were prepared from mouse thymus, spleen, and lymph nodes, and stained with fluorochrome-conjugated antibodies by standard techniques. Pancreas-infiltrating leucocytes were isolated as follows: after removal of pancreatic lymph nodes, whole pancreas was minced finely and sequentially digested at 37°C in 1 ml DMEM media containing 1 mg/ml collagenase IV for 1 min, at 0.5 mg/ml for 10 min, and at 0.2 mg/ml for 5 min, with collection of suspended calls at each step. For analysis of early thymic and bone marrow subsets (Figure 1D and E; Supplementary Figure S1C), T-cell precursors were identified by gating on cells with no expression of CD3, CD4, CD8, NK1.1, Mac-1, Gr-1, B220, or Ter119 (i.e lin$^-$). Within the lin$^-$ population, DN1-DN4 stages were identified by expression of CD25 and CD44, and the CLP population was identified by expression of IL7Rα, c-Kit, and Sca-1. Analytical flow cytometry was performed using a FACS Calibur flow cytometer (BD). Data processing for presentation was done using FlowJo 7.5 (Treestar Inc.). Cell sorting was performed using the BD FACS-Aria.

Microarray analysis

Both the previously published gene expression data used for comparison in this work (Kasler *et al*, 2011) and the new data are archived in the GEO database (http://www.ncbi.nlm.nih.gov/geo/) under accession number GSE26488. DP thymocytes were isolated from three littermate pairs of OT-2 and OT-2, HDAC7-ΔP TG animals injected with agonist peptide (chicken ovalbumin, residues 323–339, 200 μl i.p., 50 μM solution in PBS) 2.5 h previously. Total RNA was prepared from thymocytes using the RNeasy kit (Qiagen). Array probes were prepared using the Affymetrix GeneChip WT labelling system, and hybridized to Affymetrix mouse Gene 1.0 ST arrays. Arrays were scanned using an Affymetrix GCS3000 scanner and the GCOS 1.4 data acquisition software, and data were normalized using RMA in Affymetrix Expression Console. Significant differential expression was scored using the Stanford University SAM analysis package (Tusher *et al*, 2001). Significance was assessed using the 2-class permuted *t*-test method. Genes were scored as differentially expressed based on a SAM score of >1.85 and a mean fold differential expression value of 1.5.

Northern and western blotting

DP thymocytes for western blotting from Ova peptide-injected mice were prepared by FACS. For *ex vivo* activation, thymocytes were isolated by magnetic bead sorting for CD8 expression, followed by 2 h resting in RPMI/10% FBS. Cells were then plated at 2×10^6 cells/ml, with 2 μg/ml α-CD28, in 6-well dishes coated overnight at 4°C with α-CD3 (10 μg/ml). Cell lysates were prepared using RIPA buffer with protease and phosphatase inhibitors (Sigma). For assay of autoantibodies, tissue extracts were prepared from B6/Rag1$^{-/-}$ mice using 1% SDS containing 0.2 M Tris–HCl (pH 6.8) with protease inhibitors (Sigma). After SDS–PAGE, proteins were transferred onto nitrocellulose membranes, and blocked in TBS, 0.1% Tween-20 (TBS/T), 4.0% BSA. Sera were incubated with membranes at 1:250 dilution. After incubation with HRP- or IRDye- (LiCor) conjugated antibodies, signal was detected using chemiluminescence and film or a LiCor Odyssey scanner, respectively. For quantitative western analysis shown in Supplementary Figure S3B and Figure 4B, films were optically scanned. For Figure 4D and E, membranes were scanned with a LiCor Odyssey scanner. Bands were quantified using ImageJ (Wayne Rasband, National Institutes

of Health). For northern blotting, total RNA was prepared from thymocytes using Trizol. RNA (15 μg/lane) was resolved by formaldehyde agarose electrophoresis and transferred onto charged nylon membranes. Membranes were hybridized with ^{32}P end-labelled DNA oligonucleotide probe, washed, exposed to storage phosphor screens (Fuji), and imaged using a Molecular Imager FX scanner (Bio-Rad). Northern probe sequences were as follows: GAPDH: 5′-gtcattgaga gcaatgccag ccccggcatc gaaggtggaa-3′. Nor-1: 5′-agcttcaggt agaagatgcg ctggaggccc tgggtacaga-3′. GADD45β: 5′-tctcagtctc ctcttgcctg aggtgccctc cttccgacct-3′.

Adoptive transfer of lymphocytes

T and B cells were isolated from spleens of HDAC7-ΔP and littermate control mice using magnetic beads (Miltenyi). $Rag1^{-/-}$ recipients (8 for each group) were injected via tail vein with 5×10^6 WT B cells alone, 5×10^6 WT B cells together with 5×10^6 HDAC7-ΔP T cells, 5×10^6 WT B cells together with 5×10^6 littermate control T cells, or 5×10^6 WT B cells together with 2.5×10^6 HDAC7-ΔP and 2.5×10^6 littermate control T cells. Recipients were weighed weekly. Loss of 20% of starting body weight was treated as a study end point. Faecal samples were collected weekly and fatty acid quantified by $CHCl_3$-MeOH extraction, followed by $K_2Cr_2O_7/H_2SO_4$ treatment and OD measurement at 450 nm.

Haematopoietic chimeras

Recipients (8- to 10-week-old BoyJ) mice were irradiated with a split dose of 700 + 500 Rads, 3 h apart, from a ^{137}Cs source (J.S. Shepherd and Associates). Mice were reconstituted with 5×10^6 bone marrow cells from WT (CD45.1/.2 heterozygote) or HDAC7-ΔP TG (CD45.2) donors, injected retro-orbitally in 200 μl of PBS.

Histology/immunofluorescence imaging

For histology, animals were trans-cardially perfused with PBS followed by PBS/3% paraformaldehyde (PFA), fixed 18 h at 4°C in PBS/3% PFA, then stored in 70% EtOH. Paraffin-embedded tissues were sectioned and H-E stained according to standard protocols. Histologic images were acquired using a Zeiss Axio Observer.z1 microscope. For IF imaging, Frozen tissue sections from perfused/fixed mice were further acetone-fixed, washed with PBS/T, blocked with PBS/T + 1% BSA, and incubated overnight at 4°C with diluted (1:50 in PBS) sera as indicated (Figure 5C). Slides were incubated with Alexa 488-conjugated α-mouse secondary antibodies in PBS + 1% BSA, followed by TOPRO3 dye in PBS. Slides were images acquired with a Leica TCS SP5 laser-scanning confocal microscope.

Assay of ex vivo proliferation and Treg function

To assess Treg function, WT and HDAC7-ΔP splenic $CD4^+CD25^{hi}$ Treg cells were sorted by FACS. $CD4^+CD25^-CD44^-CD69^-$ responder cells were isolated from Boy/J mice using magnetic beads. CFSE-labelled responder cells (5×10^4) were added to 96-well plates with a 1:1 mixture of αCD3 and αCD28 microbeads (Invitrogen) as well as the indicated number (Supplementary Figure S2A) of $CD4^+CD25^{hi}$ suppressor cells. After 3 days, cells were stained for CD4 and CD45.1 to distinguish responders and suppressors, and analysed by flow cytometry. To assay *ex vivo* proliferation of OT-2/HDAC7-ΔP cells, splenocytes were prepared from OT-2 and OT-2/HDAC7-ΔP mice, CFSE labelled and cultured at 5×10^6/ml in RPMI/5% FBS supplemented with 20 U/ml IL-2 and 0.5 μM $Ova_{323–339}$. Surface marker expression and CFSE dilution were measured by flow cytometry at indicated intervals (Supplementary Figure S2G and H).

Supplementary data

Supplementary data are available at *The EMBO Journal* Online (http://www.embojournal.org).

Acknowledgements

We thank John Carroll and Teresa Roberts for figure preparation, Caroline Miller and Jo Dee Fish for histological tissue preparation and staining, and Linda Ta for DNA microarray hybridization and image acquisition.

Author contributions: HK wrote the manuscript, conceived of experiments, and performed experiments. HWL and DM conceived of experiments and performed experiments. AC and IL performed experiments and provided other technical support. EV supervised the work, wrote the manuscript, and conceived of experiments.

Conflict of interest

The authors declare that they have no conflict of interest.

References

Anderson MS, Todd JK, Glode MP (2005a) Delayed diagnosis of Kawasaki syndrome: an analysis of the problem. *Pediatrics* **115:** e428–e433

Anderson MS, Venanzi ES, Chen Z, Berzins SP, Benoist C, Mathis D (2005b) The cellular mechanism of Aire control of T cell tolerance. *Immunity* **23:** 227–239

Anderson MS, Venanzi ES, Klein L, Chen Z, Berzins SP, Turley SJ, von Boehmer H, Bronson R, Dierich A, Benoist C, Mathis D (2002) Projection of an immunological self shadow within the thymus by the aire protein. *Science* **298:** 1395–1401

Barnden MJ, Allison J, Heath WR, Carbone FR (1998) Defective TCR expression in transgenic mice constructed using cDNA-based alpha- and beta-chain genes under the control of heterologous regulatory elements. *Immunol Cell Biol* **76:** 34–40

Bennett CL, Brunkow ME, Ramsdell F, O'Briant KC, Zhu Q, Fuleihan RL, Shigeoka AO, Ochs HD, Chance PF (2001a) A rare polyadenylation signal mutation of the FOXP3 gene (AAUAAA–>AAUGAA) leads to the IPEX syndrome. *Immunogenetics* **53:** 435–439

Bennett CL, Christie J, Ramsdell F, Brunkow ME, Ferguson PJ, Whitesell L, Kelly TE, Saulsbury FT, Chance PF, Ochs HD (2001b) The immune dysregulation, polyendocrinopathy, enteropathy, X-linked syndrome (IPEX) is caused by mutations of FOXP3. *Nat Genet* **27:** 20–21

Bluthmann H, Kisielow P, Uematsu Y, Malissen M, Krimpenfort P, Berns A, von Boehmer H, Steinmetz M (1988) T-cell-specific deletion of T-cell receptor transgenes allows functional rearrangement of endogenous alpha- and beta-genes. *Nature* **334:** 156–159

Bouillet P, Metcalf D, Huang DC, Tarlinton DM, Kay TW, Kontgen F, Adams JM, Strasser A (1999) Proapoptotic Bcl-2 relative Bim required for certain apoptotic responses, leukocyte homeostasis, and to preclude autoimmunity. *Science* **286:** 1735–1738

Bouillet P, Purton JF, Godfrey DI, Zhang LC, Coultas L, Puthalakath H, Pellegrini M, Cory S, Adams JM, Strasser A (2002) BH3-only Bcl-2 family member Bim is required for apoptosis of autoreactive thymocytes. *Nature* **415:** 922–926

Calnan BJ, Szychowski S, Chan FK, Cado D, Winoto A (1995) A role for the orphan steroid receptor Nur77 in apoptosis accompanying antigen-induced negative selection. *Immunity* **3:** 273–282

Chang S, McKinsey TA, Zhang CL, Richardson JA, Hill JA, Olson EN (2004) Histone deacetylases 5 and 9 govern responsiveness of the heart to a subset of stress signals and play redundant roles in heart development. *Mol Cell Biol* **24:** 8467–8476

Chang S, Young BD, Li S, Qi X, Richardson JA, Olson EN (2006) Histone deacetylase 7 maintains vascular integrity by repressing matrix metalloproteinase 10. *Cell* **126:** 321–334

Cheng LE, Chan FK, Cado D, Winoto A (1997) Functional redundancy of the Nur77 and Nor-1 orphan steroid receptors in T-cell apoptosis. *EMBO J* **16:** 1865–1875

Daniels MA, Teixeiro E, Gill J, Hausmann B, Roubaty D, Holmberg K, Werlen G, Hollander GA, Gascoigne NR, Palmer E (2006) Thymic selection threshold defined by compartmentalization of Ras/MAPK signalling. *Nature* **444:** 724–729

Dequiedt F, Kasler H, Fischle W, Kiermer V, Weinstein M, Herndier BG, Verdin E (2003) HDAC7, a thymus-specific class II histone deacetylase, regulates Nur77 transcription and TCR-mediated apoptosis. *Immunity* **18:** 687–698

Fife BT, Bluestone JA (2008) Control of peripheral T-cell tolerance and autoimmunity via the CTLA-4 and PD-1 pathways. *Immunol Rev* **224:** 166–182

Gehart H, Kumpf S, Ittner A, Ricci R (2010) MAPK signalling in cellular metabolism: stress or wellness? *EMBO Rep* **11:** 834–840

Grozinger CM, Schreiber SL (2000) Regulation of histone deacetylase 4 and 5 and transcriptional activity by 14-3-3-dependent cellular localization. *Proc Natl Acad Sci USA* **97:** 7835–7840

Hildeman DA, Zhu Y, Mitchell TC, Bouillet P, Strasser A, Kappler J, Marrack P (2002) Activated T cell death *in vivo* mediated by proapoptotic bcl-2 family member bim. *Immunity* **16:** 759–767

Hori S, Nomura T, Sakaguchi S (2003) Control of regulatory T cell development by the transcription factor Foxp3. *Science* **299:** 1057–1061

Hutcheson J, Scatizzi JC, Siddiqui AM, Haines 3rd GK, Wu T, Li QZ, Davis LS, Mohan C, Perlman H (2008) Combined deficiency of proapoptotic regulators Bim and Fas results in the early onset of systemic autoimmunity. *Immunity* **28:** 206–217

Kao HY, Verdel A, Tsai CC, Simon C, Juguilon H, Khochbin S (2001) Mechanism for nucleocytoplasmic shuttling of histone deacetylase 7. *J Biol Chem* **276:** 47496–47507

Kasler HG, Young BD, Mottet D, Lim HW, Collins AM, Olson EN, Verdin E (2011) Histone deacetylase 7 regulates cell survival and TCR signaling in CD4/CD8 double-positive thymocytes. *J Immunol* **186:** 4782–4793

Keir ME, Freeman GJ, Sharpe AH (2007) PD-1 regulates self-reactive CD8+ T cell responses to antigen in lymph nodes and tissues. *J Immunol* **179:** 5064–5070

Lu J, McKinsey TA, Nicol RL, Olson EN (2000) Signal-dependent activation of the MEF2 transcription factor by dissociation from histone deacetylases. *Proc Natl Acad Sci USA* **97:** 4070–4075

McKinsey TA, Zhang CL, Olson EN (2001) Identification of a signal-responsive nuclear export sequence in class II histone deacetylases. *Mol Cell Biol* **21:** 6312–6321

Meagher C, Tang Q, Fife BT, Bour-Jordan H, Wu J, Pardoux C, Bi M, Melli K, Bluestone JA (2008) Spontaneous development of a pancreatic exocrine disease in CD28-deficient NOD mice. *J Immunol* **180:** 7793–7803

Mihaylova MM, Vasquez DS, Ravnskjaer K, Denechaud PD, Yu RT, Alvarez JG, Downes M, Evans RM, Montminy M, Shaw RJ (2011) Class IIa histone deacetylases are hormone-activated regulators of FOXO and mammalian glucose homeostasis. *Cell* **145:** 607–621

Mosenden R, Tasken K (2011) Cyclic AMP-mediated immune regulation–overview of mechanisms of action in T cells. *Cell Signal* **23:** 1009–1016

Nagamine K, Peterson P, Scott HS, Kudoh J, Minoshima S, Heino M, Krohn KJ, Lalioti MD, Mullis PE, Antonarakis SE, Kawasaki K, Asakawa S, Ito F, Shimizu N (1997) Positional cloning of the APECED gene. *Nat Genet* **17:** 393–398

Navarro MN, Goebel J, Feijoo-Carnero C, Morrice N, Cantrell DA (2011) Phosphoproteomic analysis reveals an intrinsic pathway for the regulation of histone deacetylase 7 that controls the function of cytotoxic T lymphocytes. *Nat Immunol* **12:** 352–361

Niki S, Oshikawa K, Mouri Y, Hirota F, Matsushima A, Yano M, Han H, Bando Y, Izumi K, Matsumoto M, Nakayama KI, Kuroda N (2006) Alteration of intra-pancreatic target-organ specificity by abrogation of Aire in NOD mice. *J Clin Invest* **116:** 1292–1301

Parra M, Mahmoudi T, Verdin E (2007) Myosin phosphatase dephosphorylates HDAC7, controls its nucleocytoplasmic shuttling, and inhibits apoptosis in thymocytes. *Genes Dev* **21:** 638–643

Peter PS, Brady JE, Yan L, Chen W, Engelhardt S, Wang Y, Sadoshima J, Vatner SF, Vatner DE (2007) Inhibition of p38 alpha MAPK rescues cardiomyopathy induced by overexpressed beta 2-adrenergic receptor, but not beta 1-adrenergic receptor. *J Clin Invest* **117:** 1335–1343

Ramsey C, Winqvist O, Puhakka L, Halonen M, Moro A, Kampe O, Eskelin P, Pelto-Huikko M, Peltonen L (2002) Aire deficient mice develop multiple features of APECED phenotype and show altered immune response. *Hum Mol Genet* **11:** 397–409

Rincon M, Whitmarsh A, Yang DD, Weiss L, Derijard B, Jayaraj P, Davis RJ, Flavell RA (1998) The JNK pathway regulates the *In vivo* deletion of immature CD4(+)CD8(+) thymocytes. *J Exp Med* **188:** 1817–1830

Sabapathy K, Kallunki T, David JP, Graef I, Karin M, Wagner EF (2001) c-Jun NH2-terminal kinase (JNK)1 and JNK2 have similar and stage-dependent roles in regulating T cell apoptosis and proliferation. *J Exp Med* **193:** 317–328

Starr TK, Jameson SC, Hogquist KA (2003) Positive and negative selection of T cells. *Annu Rev Immunol* **21:** 139–176

Staton TL, Lazarevic V, Jones DC, Lanser AJ, Takagi T, Ishii S, Glimcher LH (2011) Dampening of death pathways by schnurri-2 is essential for T-cell development. *Nature* **472:** 105–109

Sugawara T, Moriguchi T, Nishida E, Takahama Y (1998) Differential roles of ERK and p38 MAP kinase pathways in positive and negative selection of T lymphocytes. *Immunity* **9:** 565–574

Tanaka S, Maeda S, Hashimoto M, Fujimori C, Ito Y, Teradaira S, Hirota K, Yoshitomi H, Katakai T, Shimizu A, Nomura T, Sakaguchi N, Sakaguchi S (2010) Graded attenuation of TCR signaling elicits distinct autoimmune diseases by altering thymic T cell selection and regulatory T cell function. *J Immunol* **185:** 2295–2305

Tivol EA, Borriello F, Schweitzer AN, Lynch WP, Bluestone JA, Sharpe AH (1995) Loss of CTLA-4 leads to massive lymphoproliferation and fatal multiorgan tissue destruction, revealing a critical negative regulatory role of CTLA-4. *Immunity* **3:** 541–547

Tusher VG, Tibshirani R, Chu G (2001) Significance analysis of microarrays applied to the ionizing radiation response. *Proc Natl Acad Sci USA* **98:** 5116–5121

Vega RB, Matsuda K, Oh J, Barbosa AC, Yang X, Meadows E, McAnally J, Pomajzl C, Shelton JM, Richardson JA, Karsenty G, Olson EN (2004) Histone deacetylase 4 controls chondrocyte hypertrophy during skeletogenesis. *Cell* **119:** 555–566

Wang AH, Kruhlak MJ, Wu J, Bertos NR, Vezmar M, Posner BI, Bazett-Jones DP, Yang XJ (2000) Regulation of histone deacetylase 4 by binding of 14-3-3 proteins. *Mol Cell Biol* **20:** 6904–6912

Wang B, Moya N, Niessen S, Hoover H, Mihaylova MM, Shaw RJ, Yates 3rd JR, Fischer WH, Thomas JB, Montminy M (2011) A hormone-dependent module regulating energy balance. *Cell* **145:** 596–606

Weant AE, Michalek RD, Khan IU, Holbrook BC, Willingham MC, Grayson JM (2008) Apoptosis regulators Bim and Fas function concurrently to control autoimmunity and CD8+ T cell contraction. *Immunity* **28:** 218–230

Woronicz JD, Calnan B, Ngo V, Winoto A (1994) Requirement for the orphan steroid receptor Nur77 in apoptosis of T-cell hybridomas. *Nature* **367:** 277–281

Zhang CL, McKinsey TA, Chang S, Antos CL, Hill JA, Olson EN (2002) Class II histone deacetylases act as signal-responsive repressors of cardiac hypertrophy. *Cell* **110:** 479–488

Zhou X, Richon VM, Rifkind RA, Marks PA (2000) Identification of a transcriptional repressor related to the noncatalytic domain of histone deacetylases 4 and 5. *Proc Natl Acad Sci USA* **97:** 1056–1061

Zucchelli S, Holler P, Yamagata T, Roy M, Benoist C, Mathis D (2005) Defective central tolerance induction in NOD mice: genomics and genetics. *Immunity* **22:** 385–396